Serbian Tribology Society

SERBIATRIB '11

12th International Conference on Tribology

Faculty of Mechanical Engineering in Kragujevac

Kragujevac, Serbia, 11 – 13 May 2011

DAMAGE OF THE Co-Cr-Mo FEMORAL HEAD OF A TOTAL HIP PROSTHESIS AND ITS INFLUENCE ON THE WEAR MECHANISM

Lucian Capitanu[1], Liliana Laura Badita[2], Dumitru Catalin Bursuc[3]
[1]Institute of Solid Mechanics of Romanian Academy, Bucharest, Romania,
[2]Micro and Nanomechatronic Technolologies Laboratory, National Institute for Research and Development in Mechatronics and Measurement Technique Bucharest, Romania, badita_l@yahoo.com
[3]Military Technical Academy, Bucharest, Romania

Abstract: *Co-Cr alloy is one of the most used alloys for artificial hip joints and offers a good combination of mechanical properties, corrosion resistance and biocompatibility. To increase its resistance to wear are commonly used hard coating thin layers of Co-Cr-Mo. Analyzing a femoral head of a Co-Cr modular total hip prosthesis coated Co-Cr-Mo, we found peeling coating, abrasion of the substrate, but and hardening of abrasion traces against subsurface initial hardness. This paper presents an analysis by the Student test, of the microhardness peeling a portion of a scratch from a femoral head explant covered with Co-Cr-Mo, and that demonstrate the transformation of wear mechanism from three bodies abrasion in two bodies abrasion.*

Keywords: *total hip prostheses, Co-Cr-Mo coating, spalling, three-bodies abrasion, hardening, two-body abrasion.*

1. INTRODUCTION

Total hip prostheses are among the most successful medical devices. Sir John Charnley, the "father" of modern hip artificial joints, he called "the programmed failure medical devices", now they funcionand generally without problems in the human body for over 12-15 years. Expanding surgical procedure total hip replacement and in younger patients, with intense physical activity, required to find technical and technology solutions to increase the lifespan of total hip prosthesis. However their durability is limited by the wear resistance of the joint bearing femoral head - acetabular cup. In addition, long-term cyclic mechanical loading of the femoral head of a total hip prosthesis, leads to deformation of the femoral head [1]. Scientific and technological advances have made today will be used for a wide range of modular hip prostheses, alloy or ceramic biocompatible, very resistant to wear. If the exception the prosthesis metal / metal have recently been reconsidered, total hip prostheses most used are of the femoral head of Co-Cr-Mo alloy or Ti-6Al-4V, which acts against acetabular cups of ultra-high weight polyethylene molecular (UHMWPE).

The base material of the femoral head provides the taking over mechanical loading, and hard coating on the femoral head provides (or should) wear resistance. There are several methods of thin and multilayer coating of the femoral heads, suitable of the coating material and the substrate. The most common PVD coating process is suitable both Co-Cr-Mo alloy, and Ti-6Al-4V. Ti-6Al-4V alloy has an excellent corrosion resistance, a very high biocompatibility, high strength relative to weight and also a great tenacity, for these reasons he is an alloy widely used for advanced biomedical applications [2].

However, the tribological properties of these alloys are known to be weak, especially in abrasive and sliding conditions [3]. High friction coefficient and severe adhesive wear occurs frequently when Ti-6Al-4V alloy sliding against other engineering materials. Were studied several surface treatments to modify the tribological properties of this alloy, including plasma nitriding [4], ion implantation by plasma immersion [5], laser nitriding and physical vapor deposition (PVD) [6]. Among various processes, PVD can produce coating layers at lower temperatures of the process and therefore, it has the advantage of fewer adverse effects on mechanical properties of the substrate. In the literature many studies are present Ti-6Al-4V alloy coated with either a single coating [7,8] or by duplex approach, aimed at increasing the loading on substrate: nitration / TiN [9], HVOF WC -Co / TiN [10], nitration / DLC [11], deep hardening oxygen / DLC [12].

The friction properties of a tribosistem strongly depend of the matched material properties, the external environment and the nature of the wear particles generated during sliding [20]. The way that deforms a surface will dictate the nature of the wear particles generated, which in turn can significantly influence the wear behavior of materials. Tribofilms and wear particles generated during sliding are known to influence the behavior of the materials friction [21]. The macro-mechanical tribological mechanisms describe friction and wear phenomena by taking into account the distribution stresses - strains in the entire contact, total elastic and plastic deformations, formation process of wear debris and its dynamics [22,23].

Recently, the effect of different mating materials on friction behavior of TiN coatings with different crystallographic orientations was studied [24]. It was noted that the formation of a titanium oxide layer on the surface, lead to a lower value of friction. Much research has been aimed at studying the tribological behavior of pure titanium metal and titanium alloys [25,26]. But reports on the wear behavior of Ti thin films are rare.

Since titanium nitrides are hard biocompatible materials [27,28,29] with excellent resistance to abrasion, have been developed more advanced processing methods in order to achieve a nitrided layer on the surface of materials. At the nitriding in plasma [30], nitrogen atoms diffuse into the titanium matrix, forming a layer of TiN and Ti_2N compounds, usually followed by a deeper diffusion layer. This layered structure produces a continuous profile of hardness, thus providing adequate support of the coating [28,31]. However, the physical properties of treated surface are highly dependent on plasma coating technique and processing parameters.

Co-Cr-Mo alloy is one of the most used implant alloys for artificial joints and offers a good combination of mechanical properties, good corrosion resistance and high biocompatibility [37,38]. There are several types of materials currently used CoCrMo. Each material has a different microstructure and thus different properties optimized for a design or specific function [39]. The microstructure and alloy composition affect the corrosion behavior of simulated body fluids due to changes in surface chemistry. Hiromoto et. al., [34], observed that the passive film composition depends on the solution chemistry and limits grain growth results in a decrease of corrosion resistance of weak alloys forged Ni-Co-Cr-Mo.

It is also well known that these changes affect the mechanical properties and microstructural properties of wear [42-44]. Dobbs and Robertson [24] showed that heat treatment improved the mechanical properties of the alloy, without loss of corrosion resistance. Similarly, Cawley et. al., [43] analyzed the mechanical properties and hardness of a Co-Cr-Mo alloy heat-treated and have found a correlation between carbide volume fraction and wear rate, but they did not observe any influence on the mechanical properties.

We analyzed a series of eight total hip prosthesis with modular femoral head of Ti-6Al-4V alloy and Co-Cr alloy PVD coated with TiN and Co-Cr-Mo respectively, recovered following revision surgery, finding scratching, cracking, peeling and tribocorrosion of thin layers coating. Considering our previous experience regarding the investigation of surface state of explanted total hip prosthesis, we undertook detailed research on these recovered femoral heads.

This paper presents an analysis based on Student test of the case increase microhardness a peeling portion of the coated Co-Cr-Mo femoral head explanted of a total hip prosthesis, demonstrating the transformation of wear mechanism, by three body abrasion in two body abrasion.

2. EXPERIMENTAL METHODS

The femoral head - acetabular cup joints of eight explant total hip prostheses analyzed and presented in Figure 1, have been studied in terms of femoral head damage, which led to wear femoral cups. From beginning to be noted that all joints had various degrees of wear, some of them even catastrophic.

Figure 1. Retrieved total hip prostheses were analyzed.

The investigated hip prosthesis were numbered from left to right starting from 1 to 8. The prosthesis 1 was an alloy Ti-6Al-4V, with alumina ceramic femoral head, of 28 mm diameter.

The prostheses 2-8 were modular head femoral prosthesis with a diameter of 28 or 32 mm, Co-Cr-Mo alloy and Ti-6Al-4V with different surface coatings, polished and ground.

The prosthesis 2 was with Co-Cr alloy femoral head, coated with Co-Cr-Mo alloy, the three prosthesis has titanium alloy femoral head coated with Ti-6Al-4V, 4 prosthesis had a Co-Cr alloy head, femoral head prosthesisfive had alloy Ti-6Al-4V coated with TiN, 6 and 7 had prosthetic heads Co-Cr alloy coated with Co-Cr-Mo, and 8 had a prosthetic femoral head of 32 mm Ti alloy coated with Ti-6Al-4V. All of the prostheses had acetabular cup of high molecular weight polyethylene (UHMWPE).

Joints femoral head - acetabular cup were first photographed, investigated in terms of deviations from roundness with a profilometer Talirond Rank Taylor Hobson, Leicester, UK, and the surface microhardness was investigated with a ultrasound microdurimeter, without contact, Sonotec (KRAUTKRAMER GmbH, Germany).

Surface condition was investigated by optical microscopy, using a microscope type Epiquant (Karl Zeiss Jena GmbH, Germany) and on an atomic force microscopy NanoLaboratory AFM Probe NTEGRA NT - MDT, Russia.

3. RESULTS AND DISCUSSION.

In this paper the we refer to prosthesis no. 7, of a PVD coated Co-Cr femoral head with a layer of Co-Cr-Mo alloy, whose joint components is shown in Figure 2.

a b

Figure 2. Femoral head and acetabular cup of THP 7.

Microhardness measurements of femoral head were made circumferential on three parallel (one located at 5 mm below the pole, one at the equator and another at 5 mm below the equator) as shown in plotting of Figure 3.

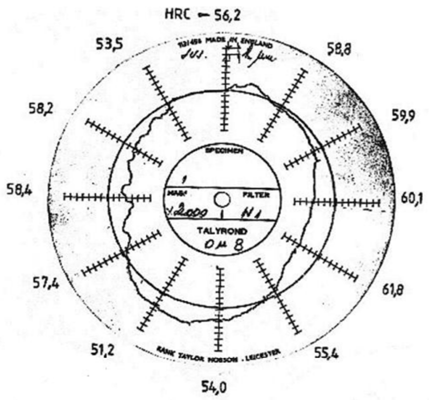

Parallel located at 5 mm below the pole

Figure 3. Femoral head surface deformation and microhardness on parallel situated at 5 mm below the pole.

Were made primarily five measurements on the flat part of the head, and their average was considered as reference value, close to the initially microhardness, because this area is less influenced by cyclical loading status. The result is a hardness of 57 HRC. The roundless records show a serious distortion of the femoral head, especially on parallel located 5 mm below the pole (Figure 3).

Note the ovoid shape of the head in the this plane with the two zones and two expanded areas, diametrically opposed. In the squeezed opposite areas, the microhardness increase in values between 58.4 and 61.8 HRC, while in the expanded areas fell to 54.0 HRC value. There are severe variations from initial microhardness, which could be due to the cold hardening material cyclc compressed.

After inspection of optical microscopy were detected coatings areas completely destroyed (Figure 4)

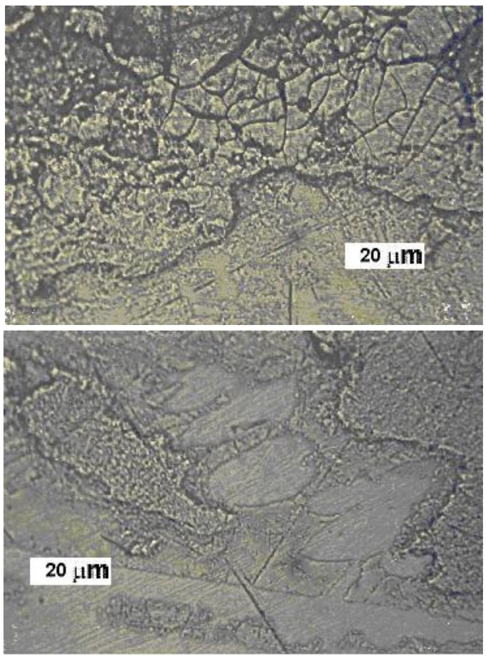

a)

b)

Figure 4. Optical microscopy images of relevant areas on the surface of the femoral head 7.

The investigation by FEM surface condition of the femoral head, showed a relatively uniform roughening of the femoral head surface, with higher R_a values, but without too much dispersion, only very few deep scratches.

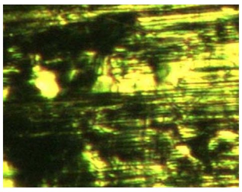
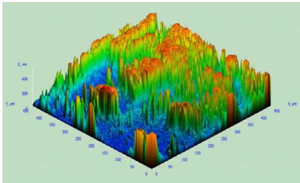

zona 6 R_a = 148.187 nm

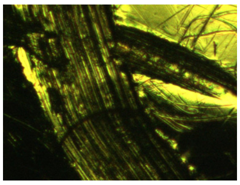
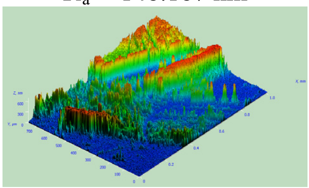

zona 15 R_a = 134.250 nm

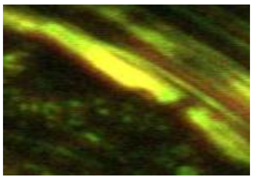
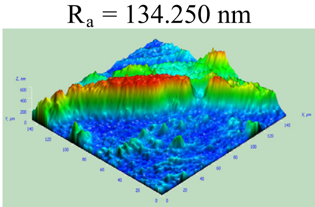

zona 16 R_a = 119,696 nm

Figure 5. Analiza unor imagini AFM - cap femural 7

R_a values for three randomly chosen areas, are 148.187 nm, 134.250 nm and 119.696 nm respectively (Figure 5). They are approximately 2.5 - 3 times higher than the initial surface Ra values of 0.05 mm, provided by ISO 7206-2, but in a more uniform range than the other studied femoral head, which was surprising.

To elucidate this finding, we used an original tribometru (Figure 6) the ball on the plan type, with reciprocal sliding motion (Figure 6b) for studying resistance of thin layers.

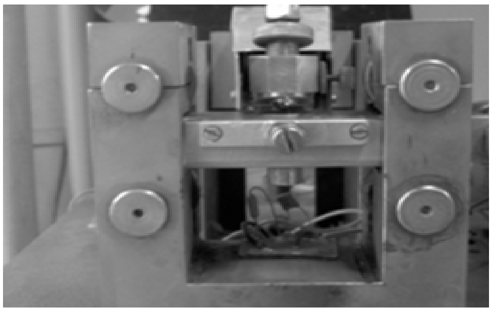

a)

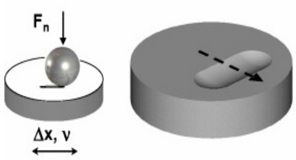

b

c

Figure 6. Tribometer ball on plane, with sliding reciprocal movement (a), the scheme of motion (b) and one of the samples used (c).

I tested with this tribometer five disk samples C120 alloy with HRC 59 hardness and Rp 3 tool steel with hardness 62 HRC. The alumina ball was 6 mm in diameter, with higher hardness than the tested materials. They used loads of 1-5 N, to have various contact efforts, at a speed of 1, 85 cm / s.

Was quantify the volume of material removed by wear, using the "imprint method", imprint length split into ten equal parts, mathematic calculation of each wear sector based on the transverse profile of the imprints in this area, averaging these sectoral volume of material removed by wear, and by dividing the length of the test or friction course, determining the wear rate (mm / h or mm / km). Initial growth was observed between 1 and 2 N load, followed by a sudden drop of it between 2 and 4 N, then the decline has almost flattened. Before carrying out the wear tests, a check was made of the distribution normality of hardness measurements. For this purpose we made on each sample every 36 indentation at loads of 1-5 N. Microhardness imprints were made by Vickers method, using a PMT 3 microdurimeter. Imprints were made at equal distances inside a square with sides of 0.5 mm, as shown in Figure 7.

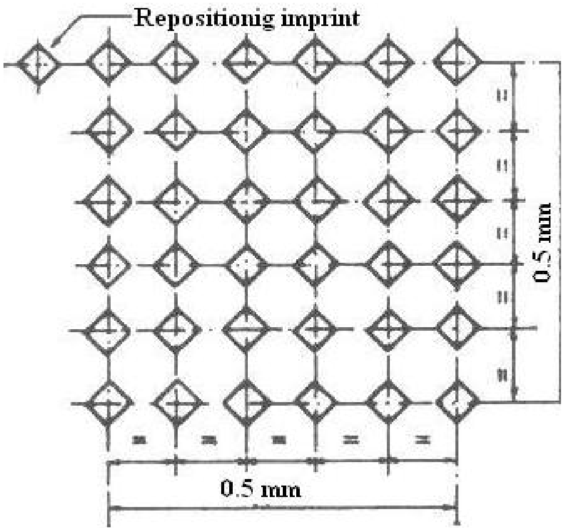

Figure 7. Schema location of microhardness imprints made with an microdurimeter PMT 3.

Microhardness values measured on a sample of C 120 steel, hardened to 62 HRC are shown in table 1, in the order they appear in the field that were performing the tests. To check the normality of the distribution microhardness values, we used Shapiro - Wilk test [13]. This test, based on order statistics is for the verification very small selections of ($3 \le n \le 50$) in terms of normality. Applying this test requires first ordering feature values, upwards, between the minimum value x_i and maximum value x_n:

$$x_1 \le x_2 \le x_3 \le ..... \le x_n \quad (1)$$

Table 1 shows the microhardness values of the field study.

Table 1. Microhardness values of studied field.

660	636	686	713	686	648
670	670	686	629	686	629
686	670	686	694	728	648
660	660	648	670	694	694
686	670	660	713	670	713
636	660	670	660	648	694

Ordering microhardness values presented in Table 1, we obtain the following sequence of order statistics:

629	629	636	636	636	648	648	648	648
660	660	660	660	660	660	670	670	670
670	670	670	670	686	686	686	686	686
686	694	694	694	694	713	713	713	728

Calculated average and dispersion of above values, was obtained:

$$\bar{x} = \frac{1}{n}\sum_{i=1}^{n} x_i = \frac{1}{36}\sum_{i=1}^{36} x_i = 671.3055 \quad \text{si} \qquad (2)$$

$$S^2 = \sum_{i=1}^{n}\left(x_i - \bar{x}\right)^2 = \sum_{i=1}^{36}\left(x_i - \bar{x}\right)^2 = 22{,}054 \qquad (3)$$

W_{calc} test statistic was calculated in accordance with equation (10) [13]:

$$W_{calc} = b^2 / S^2, \qquad (4)$$

where b is expressed as:

$$b = a_n\left(x_n - x_1\right) + a_{n-1}\left(x_{n-1} - x_2\right) + \ldots\ldots + a_{n-k+1}\left(x_{n-k+1} - x_k\right) \qquad (5)$$

In equation (5), $k = n / 2 = 16$ (for n even), and coefficients a_n, a_{n-1} ... a_{n-k+1} depend on the size of selection and are tabulated [13]. Calculation of test statistics is shown in Table 2. On the basis of relation (5) and data from Table 2, results:

$$b^2 = (146)^2 = 21529.89$$

Table 2. Calculul statisticii testului Shapiro – Wilk.

i	x_{n-k+1}	x_k	$\omega_k = x_{n-k+1} - x_k$	σ_{n-k+1}	$\sigma_{n-k+1} \cdot \omega_k$
1	728	629	99	0,4068	40,28
2	713	629	84	0,2813	23,63
3	713	636	77	0,2410	18,56
4	713	636	77	0,2121	16,34
5	694	636	58	0,1883	10,93
6	694	648	46	0,1678	7,72
7	694	648	46	0,1496	6,88
8	694	648	46	0,1331	6,13
9	686	648	38	0,1179	4,48
10	686	660	38	0,1036	3,94
11	686	660	26	0,0900	2,34
12	686	660	26	0,0770	2,02
13	686	660	26	0,0645	1,68
14	686	660	26	0,0523	1,36
15	670	660	10	0,0404	0,41
16	670	670	0	0,0287	0
17	670	670	0	0,0172	0
18	670	670	0	0,0057	0
Σ	-	-	-	-	146,70

Table 3. Determination of microhardness on the samples disk alloy C 120.

Load (N)	SAMPLE HARDNESS					IMPRINT HARDNESS				
	d (div.)	H_i	H_{med}	$H_{med} - H_i$	$\sigma_{H med}$	d (div.)	H_i	H_{med}	$H_{med} - H_i$	$\sigma_{H med}$
		(N / mm^2)					(N / mm^2)			
1	488	788		8		491	769		6	
1	479	808		28		488	779		4	
1	494	760	780	20	± 11.2	492	766	775	9	± 3.41
1	498	748		32		486	785		10	
1	483	795		15		489	775		0	
2	498	775		22		462	869		2	
2	473	829		32		465	858		9	
2	473	829	797	32	± 14.4	441	873	867	6	± 4.80
2	483	795		2		459	880		13	
2	495	757		40		466	854		13	
3	483	795		4		489	775		7	
3	468	847		56		488	779		3	
3	498	748	791	43	± 17.9	490	772	782	10	± 5.29
3	495	757		34		487	782		0	
3	479	808		17		481	802		20	
4	482	798		5		602	512		17	
4	465	859		65		580	551		22	
4	496	754	793	39	± 19.7	600	515	529	14	± 11.2
4	497	751		42		575	561		32	
4	480	805		12		605	507		22	
5	485	788		7		580	551		28	
5	481	892		7		595	524		1	
5	390	772	795	23	± 7.82	575	561	523	38	± 15.0
5	479	808		14		525	476		47	
5	477	815		20		600	515		8	

Table 4. Determination of microhardness on the samples disk steel Rp 3.

Load (N)	SAMPLE HARDNESS					IMPRINT HARDNESS				
	d (div.)	H_{i}	H_{med}	$H_{\text{med}} - H_{\text{i}}$	$\sigma_{H\ \text{med}}$	d (div.)	H_{i}	H_{med}	$H_{\text{med}} - H_{\text{i}}$	$\sigma_{H\ \text{med}}$
		(N / mm^2)					(N / mm^2)			
1	489	775	775	0	± 3.40	486	785	766	19	± 14.0
1	492	766		9		488	779		13	
1	488	779		4		498	748		18	
1	491	769		6		482	798		32	
1	486	785		10		507	721		45	
2	510	713	745	32	± 24.8	520	686	745	59	± 26.2
2	485	788		43		487	782		37	
2	476	818		73		482	798		53	
2	508	719		26		485	788		43	
2	520	686		59		525	673		72	
3	486	785	766	19	± 14.0	500	742	697	45	± 18.3
3	488	779		13		520	686		11	
3	498	748		18		531	658		39	
3	482	798		32		503	733		36	
3	507	721		45		532	655		42	
4	497	748	780	32	± 11.2	540	636	674	38	± 17.5
4	423	788		8		641	634		40	
4	483	795		15		517	694		20	
4	479	808		28		523	678		4	
4	494	760		20		505	727		53	

For the test statistics, results in accordance with equation (5), the value:

$$W_{calc} = 21520.89 / 22054 = 0,976$$

The test statistics W_{calc} is between the values $W_{0.50} = 0.970$ and $W_{0.90} = 0.984$ of the statistics Shapiro - Wilk test, for normality checking [13].

The above two values correspond to the normality of the distribution probability of 50% and 90%. By performing a linear interpolation of value W_{calc} between values $W_{0.50}$ and $W_{0.90}$, results for the probability of a normal distribution of microhardness, the value:

$$p = 0.50 + (0.90 - 0.50)\frac{0.976 - 0.970}{0.984 - 0.970} = 0,67.$$

Therefore, it can be appreciated that the values obtained by microhardness imprints belong to a 67% probability of a normal distribution, because the condition W_{067} $W_{0.50}$ is satisfied. The specimens of alloy C 120 and Rp 3 steel ones, such as having verified normal distribution, the values of microhardness, were conducted the wear tests, at normal sarcuni ranging between 1 and 5 daN.

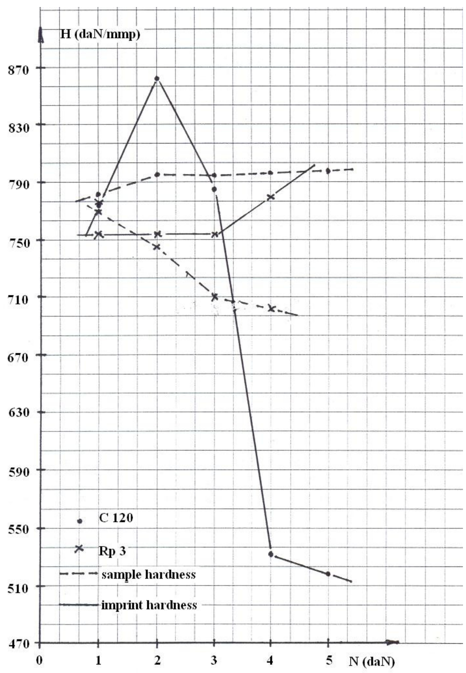

Figure 8. Microhardness variation between contact area and normal load.

On the results wear imprints and on unused portion of the samples were then conducted with five microhardness measurements at equal distances from each other, calculating both microhardness average and standard deviation.

The results are presented in Tables 3 and 4. On this basis, in Figure 8 is illustrated the correspondence between the variation of microhardness contact area of the metallic specimen, function of normal load. Figure 8 illustrates a relatively quick increasing of contact area initial hardness, which results in a low wear rate, until a certain load (contact pressure), then show a sharp decreasing.

The analysis presented above illustrates that the action of normal load (contact pressure), causing cold hardening of metallic material. This happens only to a certain amount of contact stress, then harden layer is destroyed, and the wear rate increases catastrophically. We believe that the same phenomenon happens when explanted the femoral head of total hip prosthesis subject of this paper.

4. CONCLUSION

Due to strong cyclic loading during the patient's current activities (eg the resulting force is about four times the body weight), femoral head is subjected to cyclic deformation plus the aggressive action of the body fluid. As a result, due to the relative speed between head and cup, the wearing process takes place, amid tribocorrosion cracking induced by synovial fluid.

Tribocoroziunea occurs in the micropores and microcracks in hard coating Co-Cr-Mo, exfoliation resulting in the appearance of wear particle. They promote abrasive wear mechanism that leads to three bodies grinding thin coating of the femoral head.

We believe that the small particles resulting from wear damage coating are embedded in the cup bearing surface, still acting as a tool for grinding outer spherical surface, strong loading of femoral head and cold hardening the substrate. In this way the mechanism of wear of the femoral head surface is transformed from three-body abrasion, in a two-body abrasion process, the acetabular cup acts as an outer spherical grinding tool with abrasive particles embedded in the ultra high molecular weight polyethylene surface. Also consider that insufficient adherence to the thin film coating to base material, favors the tribocorossion cracking and peeling coating.

We believe that in case of Co-Cr alloy, strong mechanical loading of femoral head surface leads to cold hardening began of the base material (Co-Cr). This causes a relatively mild wear of coating, manifested by tarnishing it.

REFERENCES

[1] Capitanu L., Onisoru J., Iarovici A., Tiganesteanu C. Scratching mechanisms of hip artificial joints, Journal of the Balkan Tribology Associatiation, Vol. 15, No. 2, 280-291, 2009.

[2] Osterle W, Klaffke D, Griepentrog M, Gross U, Kranz I, Knabe Ch. Potential of wear Resistant coatings on Ti–6Al–4V for Artificial hip joint bearing surfaces. Wear 2008; 264:505–17.

[3] Wilson A D, Leyland A, Matthews A. A comparative study of the influence of plasma treatments PVD coatings and ion implantation On the tribological performance of Ti–6Al– 4V. Surf Coat Technol 1999; 114:70 – 80.

[4] Bemporad E, Sebastiani M, Staia M H, Puch I Cabrera E. Tribological studies on PVD / HVOF duplex coatings on Ti6Al4V substrate.Surf Coat Technol 2008; 203:566–71.

[5] Avelar-Batista J C, Spain E, Fuentes G G, Sola A, Rodriguez R, Housden J. Triode Plasma Nitriding and PVD coating: a successful pre-Treatment combination to improve the wear resistance of DLC coatings on Ti6Al4 alloy. Surf Coat Technol 2006; 201:4335–40.

[6] Zhang Z X, Dong H, Bell T, Xu B S. The effect of deep-case oxygen hardening on the Tribological Behaviour of a-C:HDLC Coatings on Ti6Al4V alloy. JAlloys Compd 2008; 464:519–25.

[7] Varenberg M., Halperin G., Etsion I., Different aspects of the role of wear debris in fretting wear, Wear 252 (2002) 902–910.

[8] Zhou Z., Rainforth W.M., Tan C.C., Zeng P., Ojeda J.J., Romero-Gonzalez M.E., Hovsepian P.Eh., The role of tribofilm and roll-like debris in the wear of nanoscale nitride PVD coatings, Wear 263 (2007) 1328–1334.

[9] Holmberg K., A concept for friction mechanisms of coated surfaces, Surf. Coat. Techn. 56(1992) 1-10.

[10] Holmberg K, Matthews A., Ronkainen H.,Coatings tribology-contact mechanisms And surface design, Tribol. Int. 31 (1998) 107–120.

[11] Tanno Y., Azushima A., Effect of counter materials on coefficients of friction of TiN coatings with preferred grain orientations, Wear 266 (2009) 1178– 1184.

[12] Valero Vidal C, Igual-Munoz A. Corrosion Science 2008; 50:1954–61.

[13] Chelliah N., Kailas S.V., Synergy between tribo-oxidation and strain rate response on governing the dry sliding wear behaviour of titanium, Wear 266 (2009) 704–712.

[14] Iliescu D. V., Vodo V. G., Statistics and clearances. Technical Press, Bucharest, 1977 (in Romanian).